



Effect of the Variation of Film Thickness on the Properties of Multilayered Si-Doped Diamond-Like Carbon Films Deposited on SUS 304, Al and Cu Substrates

An Li, Qingchun Chen, Guizhi Wu, Xin Huang, Yunfeng Wang, Zhibin Lu, Guangang Zhang, and Xiangfan Nie

Submitted: 27 April 2020 / Revised: 30 August 2020 / Accepted: 3 October 2020 / Published online: 18 November 2020

Multilayered Si-doped DLC film with thicknesses of 5.5, 10.1, 21.8 and 28.3 μm was deposited on stainless steel, aluminum alloy and copper alloy substrates by plasma-enhanced chemical vapor deposition. The mechanical and tribological properties of multilayered Si-doped DLC films deposited on three different substrates were evaluated in this study. The hardness of the multilayered Si-doped DLC film of different substrates is related to the substrate material and internal stress. In a scratch test, the adhesion of the multilayered Si-doped DLC film increased with the film thickness. The multilayered Si-doped DLC film with a thickness of 28.3 μm on stainless steel substrate has the highest adhesion of 31 N. The adhesion of the multilayered Si-doped DLC film with different thicknesses on the copper alloy is relatively poor. The ball-on-disk friction test results show that the multilayered Si-doped DLC film with thicknesses of 5.5 and 10.1 μm is prone to shear deformation and exhibit high friction coefficient. The uneven stress distribution and surface deformation of the multilayered Si-doped film deposited on the aluminum alloy and the copper alloy cause the fluctuation and rise of the friction coefficient. The wear resistance of multilayered Si-doped DLC films on different substrates is related to stress shielding and adhesion strength.

Keywords mechanical properties, multilayered Si-doped DLC film, thicknesses, tribology

1. Introduction

Stainless steel, aluminum and copper alloys are based on their excellent corrosion resistance, good processability, high electrical conductivity and high-cost performance, making them the most widely used metal materials in industrial production and living applications. However, their low hardness and poor wear resistance are one of the main causes of material loss. These shortcomings can be overcome by depositing diamond-like carbon (DLC) films with unique properties on the substrate surface (Ref 1-3). DLC films have attracted wide attention in the academia for their unique properties such as high hardness, excellent friction properties, optical transparency and superior

corrosion resistance (Ref 4-8). As a new type of hard film material, DLC can be widely used in mechanical, optical, medical and other fields and has a good application prospect.

Recently, the thickness of films is an important parameter that often plays a decisive role in these applications (Ref 9-11). However, the thickness of the conventional DLC film (3-5 μm) limits their requirements for high-load, high-speed and long service life. High residual stress is a major factor in film delamination and failure. Stress accumulation is proportional to the thickness of the deposited films, which makes it difficult to obtain a thick film (Ref 12, 13). In addition, the intrinsic stress of the DLC film and the thermal stress caused by the mismatch between the film and the substrate are the main components of the residual stress (Ref 14). The difference between the coefficient of thermal expansion (CTE) of DLC film ($2.3 \times 10^{-6}/\text{K}$) and the stainless steel ($15 \times 10^{-6}/\text{K}$), aluminum alloy ($23.5 \times 10^{-6}/\text{K}$) and copper alloy ($17 \times 10^{-6}/\text{K}$) is one of the difficulties in effectively depositing DLC film on the substrate material. Furthermore, the poor affinity between alloy and DLC film results in weak adhesion strength (Ref 15). The hardness between the substrate and the film is inconsistent and the adhesion is poor, which greatly reduces the abrasion resistance and durability of the film (Ref 16). It has been demonstrated by previous studies that doping elements (Ref 17-20) and multilayer designs (Ref 21-23) can reduce residual stress and thus increase film thickness. The advantage of Si over other doping elements is that no π bonds are formed and therefore no sp^2 bonds are formed. Moreover, the energy of the Si-C bond (3.21 eV) is smaller than the C-C bond (3.70 eV) (Ref 24), and the carbon bond distortion relaxation of the DLC film after Si doping reduces the internal stress (Ref 25). In our previous work, multilayered Si-doped DLC film that was deposited from two different Si content DLC layers had been successfully deposited on steel substrate by PECVD (Ref 26, 27). The low Si content DLC layer exhibits compressive stress,

An Li, State Key Laboratory of Solid Lubrication, Lanzhou Institute of Chemical Physics, Chinese Academy of Sciences, Lanzhou 730000, People's Republic of China; and School of Materials Science and Engineering, Lanzhou Jiaotong University, Lanzhou 730070, People's Republic of China; **Qingchun Chen**, **Guizhi Wu**, **Zhibin Lu**, and **Guangang Zhang**, State Key Laboratory of Solid Lubrication, Lanzhou Institute of Chemical Physics, Chinese Academy of Sciences, Lanzhou 730000, People's Republic of China; **Xin Huang**, School of Materials Science and Engineering, Chongqing University of Technology, Chongqing 400054, People's Republic of China; **Yunfeng Wang**, School of Materials Science and Engineering, Lanzhou Jiaotong University, Lanzhou 730070, People's Republic of China; and **Xiangfan Nie**, Science and Technology on Plasma Dynamics Laboratory, Air Force Engineering University, Xian 710038, People's Republic of China. Contact e-mails: wangyunf03@163.com and gazhang@licp.cas.cn.

and the high Si content DLC layer exhibits tensile stress. Multilayered DLC films with opposite stress can greatly reduce the stress concentration in the film system. Continuous transition in multilayer structures usually improves the bonding strength of interface and reduces thermal stress and stress jump at interface, driving force and stress intensity of crack growth (Ref 28). Various methods have been used to prepare DLC coatings. Plasma-enhanced chemical vapor deposition can control the coating thickness and structure by regulating process parameters at lower temperatures. Therefore, PECVD is suitable for coating low-melting-point aluminum alloys and copper alloys.

In this paper, multilayered DLC films with thicknesses of 5.5 to 28.3 μm were prepared on SUS 304, Al and Cu substrates by PECVD. The effects of thickness on the properties of multilayered Si-doped DLC films on different substrates were investigated. The aim of this work was to obtain thick DLC films on different substrates while maintaining high hardness, good adhesion and wear resistance.

2. Experimental Details

2.1 Film Deposition

The multilayered Si-doped DLC films with different thicknesses were deposited by the PECVD technology. (One deposition period consists of a Si_x -DLC layer with high Si content and a Si_y -DLC layer with poor Si content.) Related deposition parameters and processes had been discussed in our previous studies (Ref 27). Stainless steel, aluminum alloys and copper alloys are: SUS 304 stainless steel (0Cr19Ni9, $30 \times 30 \times 1$ mm), 3004 aluminum alloy ($30 \times 30 \times 2$ mm) and T3 copper alloy ($30 \times 30 \times 1$ mm). Their chemical compositions are given in Table 1. Firstly, stainless steel, aluminum alloy and copper alloy were mechanically polished to remove surface oxides and impurities. The substrate was ultrasonically washed in acetone and ethanol for 20 min and then dried. The samples' material was placed in the equipment and etched in argon plasma for 30 min. The Si transition layer is obtained by introducing silane into the chamber and applying a high pulse bias on the substrate to improve the adhesion to substrate. Then, multilayer structure consisting of Si_x -DLC layers and Si_y -DLC layers with different thicknesses was deposited by introducing silane and acetylene gas. The detailed parameters are listed in Table 2. The thickness of the film is achieved by regulating the number of deposition periods, which are 9, 20, 40 and 60, respectively. Four multilayered Si-doped DLC films with different deposition periods are considered in this report. More detailed description of the film deposition process and composition can be found in previous work (Ref 27, 29).

2.2 Film Characterization

Scanning electron microscopy (SEM) was used to observe the cross section and thickness of the multilayered Si-doped DLC films coated on silicon wafers. The surface curvature of the substrate before and after film deposition was measured using a FST-1000 film stress tester, and then, the residual stress of the multilayered Si-doped DLC films was calculated according to the Stoney equation. Raman spectroscopy was performed on a Raman spectrometer (LabRAM, Horiba Jobin Yvon) equipped with 532 nm exciting wavelength. The hardness (H) and Young's modulus (E) were determined according to a nanoindenter with Berkovich indenter tip. The maximum load of indentation is set at 50 mN, and the holding time is 2 s. The penetration depth of the needle is controlled within 10% of the thickness of the coating. Four replicate measurements were taken for each sample to reduce measurement error. A scratch tester (RST³, Anton Paar, Austria) was performed to study adhesion of films on different substrates. The scratch test was carried out under progressive force with a maximum load of 50 N, and the scratch morphology was observed by an optical microscope. A reciprocating ball-on-disk tester (CSM) was performed to investigate tribological properties of the films. The counterpart was YG6 ball with radius of 3 mm and hardness (HRA) of 89.5. The main component is tungsten-cobalt alloy (WC-CO) with high hardness and good wear resistance. Friction and wear experiments were carried out under the conditions of 5-mm sliding stroke, 5 Hz stroke frequency and 10 N load. After the tribological test, the wear rate of the film was investigated by a two-dimensional contact surface profiler (D-100, KLA, Tencor). The finite element method (FEM) was used to simulate the stress distribution during the ball pressure to the film. Stress distribution of multilayered Si-doped DLC films on different substrates is under external force conditions.

Table 2 The detailed parameters for depositing the multilayered Si-doped DLC films

	Gas flow (sccm)			Time (min)
	Ar	SiH_4	C_2H_2	
Si transition layer	150	50	...	15
Si_x -DLC	80	50	50	5
Si_y -DLC	150	50	150	5

Table 1 Composition of parent metals (wt.%)

Materials	Si	Mn	Cr	Ni	S	Cu	Cu+Ag	Mg	Zn	Fe	Al	As
SUS 304	≤ 1.0	≤ 2.0	17.0	8.0	≤ 0.03	Bal.
3004 Al	0.30	1.0	0.25	...	0.8	0.25	0.7	Bal.	...
T3 Cu	≤ 0.2	≤ 0.01	...	≥ 99.7	≤ 0.05	...	≤ 0.01

3. Results and Discussion

3.1 Composition and Microstructure

The typical cross-sectional SEM image of multilayered Si_x-DLC/Si_y-DLC films coated on silicon wafers with four thicknesses is shown in Fig. 1. The cross-sectional images show that the multilayered Si-doped DLC film has a distinct layered structure. The bright white and dark gray bands represent the Si_y-DLC layers and Si_x-DLC layers, respectively (Ref 30). The thickness of the Si transition layer is small and cannot be observed well in the SEM image. It can be seen that multilayered Si-doped DLC films with thicknesses of 5.5, 10.1, 21.8 and 28.3 μm can be obtained by controlling the number of deposition periods.

Figure 2 shows the residual stress of the multilayered Si-doped film of varying thicknesses deposited on silicon wafer substrates. As the film thickness increases from 5.5 to 28.3 μm, the residual stress in multilayered Si-doped DLC film increases linearly from -0.47 to -0.80 GPa. A negative bias is typically applied to the substrate during deposition, and the energy of these impinging particles is sufficient to cause particles to enter the range of several atomic layers below the formed film and to rearrange a portion of the atoms. The injection of particles below several atomic layers of the film will also cause the deposited material to swell. Further, a large amount of compressive stress is generated in the deposited film to form a tensile force on the substrate. In multilayer coatings, the heterointerface can be allowed to expand as much as possible by coherence, incoherent or semi-coherent strain, so the greater the number of interfaces, the greater the stress can be relaxed. As the film thickness increases, the stress and storage strain will increase. Although this strain energy does

not adversely affect many applications, such compressive stress can be a fatal defect in the deposition of thick films in order to prevent cracking of the film. High internal stress can cause film delamination and plastic deformation. To deposit superthick film on different substrates, the residual stress must be accurately controlled. Si-doped DLC layers having tensile and compressive stresses were obtained by changing the content of Si. In this structure, Si_x-DLC (x denotes less Si doping) exhibits compressive stress (-0.21 GPa) and Si_y-DLC (y denotes high Si content) exhibits tensile stress (0.20 GPa). Thus, the stress directions in Si_x-DLC and Si_y-DLC are opposite (Ref 27). This kind of multilayered Si-doped DLC films with coupled tensile stresses and compressive stresses can

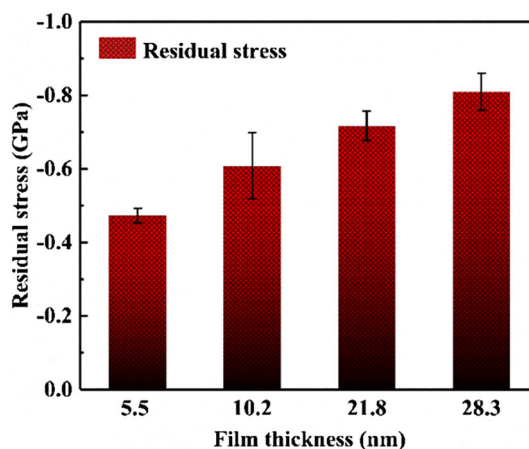


Fig. 2. Relationship between film thickness and residual stress for multilayered Si-doped DLC films with different deposition periods

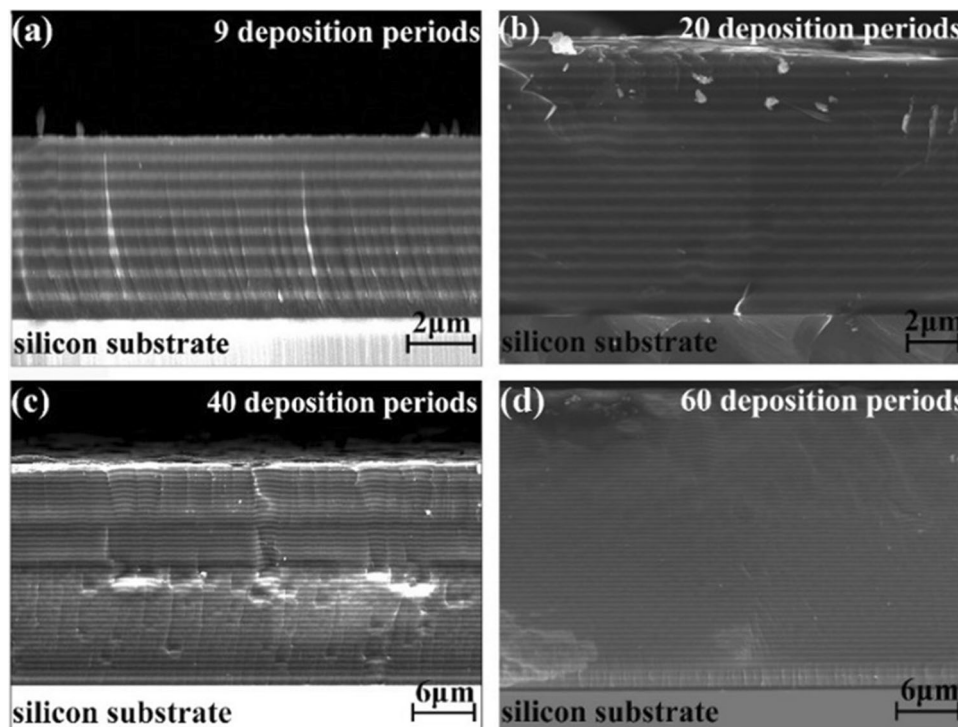


Fig. 1. Cross-sectional SEM micrographs of the multilayered Si-doped DLC films with different thicknesses: (a) 5.5 μm, (b) 10.1 μm, (c) 21.8 μm, (d) 28.3 μm

obtain as low residual stresses as possible (Ref 31). Therefore, it provides favorable conditions for the deposition of superthick DLC films on stainless steel, aluminum alloy and copper alloy substrates.

Figure 3 shows the Raman spectra of DLC films with different thicknesses on stainless steel, aluminum alloy and copper alloy substrates. An asymmetric broad peak was observed at a range between 1000 cm^{-1} and 1800 cm^{-1} for the multilayered Si-doped DLC films. The G band around 1550 cm^{-1} is attributed to the stretching model of the sp^2 carbon atom in rings or chains. The D band around 1350 cm^{-1} is due to the breathing mode of sp^2 atoms in the sixfold aromatic ring (Ref 32-34). Since the large absorption coefficient of light by carbon material, the Raman laser can only penetrate the 10-100 nm depth range of the DLC film. In view of the four different deposition periods, the thickness of the top layer of the multilayered Si-doped DLC film is greater than 200 nm. Therefore, Fig. 2 actually shows the bonding structure at the top of a multilayered Si-doped DLC film. All films have the same deposition parameters and the top is $\text{Si}_y\text{-DLC}$ layer. Therefore, the Raman spectra of multilayered Si-doped DLC films of different thicknesses on different substrates have no significant changes.

3.2 Mechanical Properties

Table 3 shows the hardness and Young's modulus of multilayered Si-doped DLC film deposited on different sub-

strates with the change of the film thickness. The hardness of films deposited on stainless-steel substrate increases with film thickness, but the elastic modulus does not increase significantly. The maximal hardness of 16.3 GPa and elastic modulus of 124 GPa are achieved, as the thickness of the film deposited on stainless steel is $28.3\text{ }\mu\text{m}$. The hardness and modulus of elasticity of multilayered Si-doped DLC films deposited on aluminum alloy substrates increase with film thickness. The films deposited on aluminum alloys have lower hardness than those deposited on stainless steel. Because the maximum penetration depth is about 600 nm, the substrate material has a slight effect on the film hardness. Generally, the increasing hardness and elastic modulus of the multilayer film are attributed to the following means. The effect of hard $\text{Si}_y\text{-DLC}$ layer in multilayers and hardening effect is caused by the large number of interfaces parallel to the substrate surface (Ref 35). However, the hardness of the multilayered Si-doped DLC film deposited on the copper substrate appears to increase initially and subsequently decrease as the film thickness increases. The hardness of the multilayered Si-doped DLC film of $10.1\text{ }\mu\text{m}$ thickness reached a maximum of 15.5 GPa. As the film thickness increased to $28.3\text{ }\mu\text{m}$, the hardness value gradually decreased to 12.3 GPa. It is worth mentioning that when the thickness of the film reaches $21.8\text{ }\mu\text{m}$, the film is partially peeled off. Therefore, the decreased hardness of the film is caused by stress release. Partial peeling occurred in the multilayered Si-doped DLC film having a thickness of more than $10\text{ }\mu\text{m}$ on copper substrate. This is because the outer d-

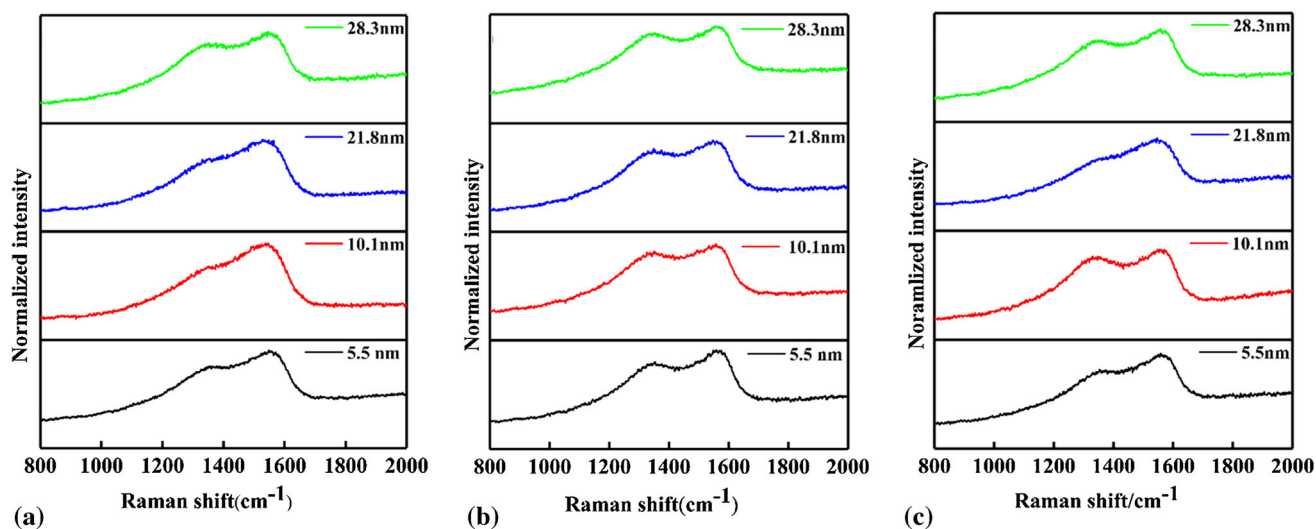


Fig. 3. Raman spectra of multilayered Si-doped DLC films with different thicknesses on different substrates: (a) stainless steel, (b) aluminum alloys and (c) copper alloys

Table 3 Nanoindentation results of multilayered Si-doped DLC films with different thicknesses on different substrates

Thickness, μm	Stainless steel		Aluminum alloys		Copper alloys	
	Hardness, GPa	Elastic modulus, GPa	Hardness, GPa	Elastic modulus, GPa	Hardness, GPa	Elastic modulus, GPa
5.5	12.7	119.3	10.6	88.3	11.9	105.7
10.1	13.1	113.1	12.3	99.5	15.5	117.8
21.8	14.4	125.7	13.4	108.7	13.5	142.6
28.3	16.3	123.4	14.5	110.5	12.3	95

orbital electrons of the Cu element are full, and it is difficult to chemically bond with the carbon element in a high-energy state. In addition, there is a large internal stress between the film and the substrate during the deposition process. Therefore, it is difficult to deposit superthick films on copper alloy substrates successfully. The ratio of H^3/E^2 is usually used to evaluate the resistance of the film to plastic deformation. The high H^3/E^2 implies a high resistance to cracks initiation and propagation,

Table 4 H^3/E^2 ratio of multilayered Si-doped DLC films with different thicknesses on different substrates

	Stainless steel, Gpa	Aluminum alloys, Gpa	Copper alloys, Gpa
9p	0.14	0.15	0.15
20p	0.17	0.18	0.27
40p	0.18	0.20	0.12
60p	0.28	0.25	0.17

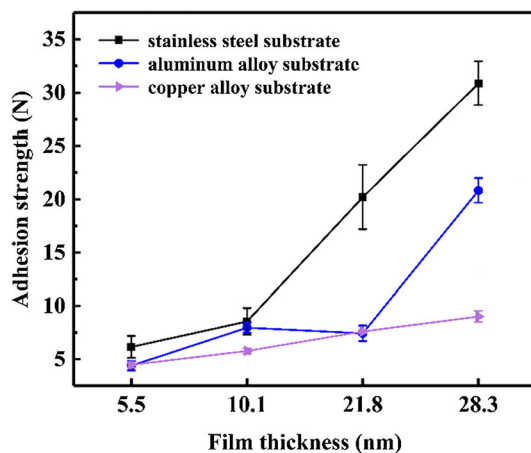


Fig. 4. Adhesion strength of multilayered Si-doped DLC films with different thicknesses deposited on different substrates

which are also desirable for wear improvement (Ref 36, 37). As shown in Table 4, the results show that the change of H^3/E^2 ratio with deposition period is similar to the change of film hardness. For H^3/E^2 , the lower the H^3/E^2 value, the worse ability to resist plastic deformation the material behaves.

Poor adhesion can directly lead to premature separation of the film from the substrate under external influence. Therefore, the adhesions of the film is critical for the practical application of the films (Ref 38, 39). Figure 4 shows the difference in adhesion (detachment from film/substrate interface) of the film deposited on stainless steel, aluminum alloy and copper alloy substrates. The adhesion of the multilayered Si-doped DLC film deposited on stainless steel, aluminum alloy and copper alloy substrates increases with film thickness. There is noticeable improvement in adhesion between the multilayered Si-doped DLC film and stainless steel as the film thickness increases compared to the other two substrates (aluminum alloy and copper alloy). With a thickness of 28.3 μm , the adhesion of the multilayered Si-doped DLC film deposited on aluminum alloy substrates is significantly improved. Moreover, the adhesion of the film deposited on the copper alloy substrate shows a slight increase with film thickness. It was not observed that the correlation between adhesion and hardness was caused by the difference of internal stress, which is a direct function of the elastic stored energy in the films. The accumulation of elastic energy storage is a factor affecting the adhesion, which is greater than the adhesive energy that can cause the film to peel off from the substrate (Ref 38, 40).

Figure 5 presents the scratch tracks of the multilayered Si-doped DLC film having a thickness of 28.3 μm deposited on stainless steel, aluminum alloy and copper alloy substrates. The wedge spalling failure of the film deposited on stainless steel occurs at a critical load of 31 N. The film produced a large number of conformal cracks before peeling off, and no cracks were formed on either side of the scratch track. This is a plastic deformation before failure, indicating that the film has good toughness. The multilayered Si-doped DLC film on aluminum alloy substrate shows buckling failure at 21 N, accompanied by curved cracks and plastic deformation. Moreover, the film was

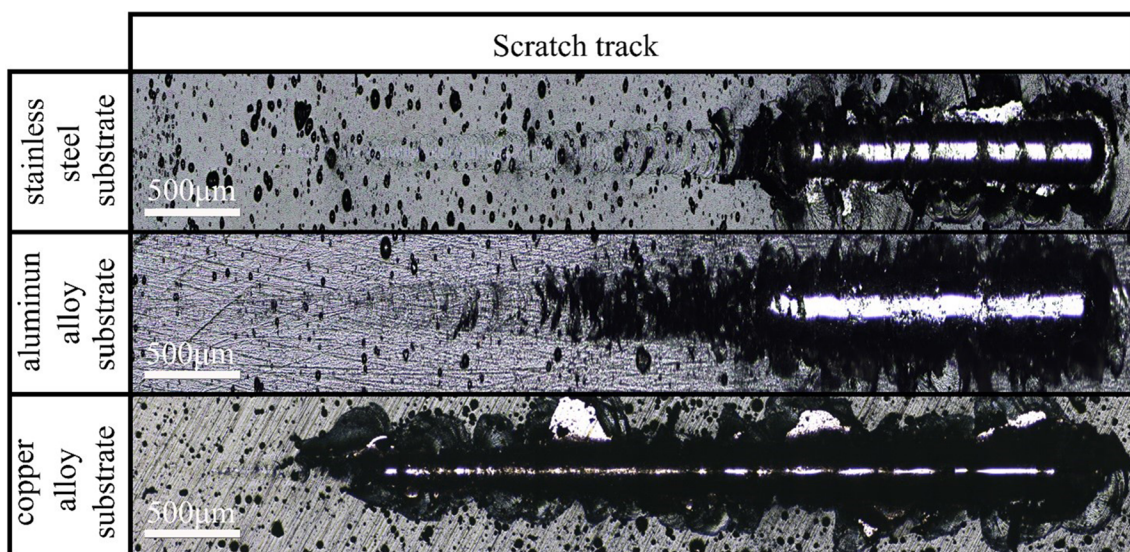


Fig. 5. Optical images of scratch track on multilayered Si-doped DLC films with a thickness of 28.3 μm deposited on stainless steel, aluminum alloy and copper alloy substrates

completely peeled off from the substrate at 30 N. From the multilayered Si-doped DLC scratch morphology on the copper alloy substrate, it can be clearly seen that the fracture failure occurred at 9 N. It is worth noting that almost no plastic deformation occurred before the film failed. It was shown that the film on the copper alloy substrate exhibits very poor plastic toughness. This may be attributed to the weak bond between Cu and C and Si, which results in the film peeling off at the interface.

3.3 Tribological Properties

The tribological properties of multilayered Si-doped DLC films with different thicknesses coated on stainless steel, aluminum alloy and copper alloy substrates were investigated by a ball-disk friction test. Figure 6 shows the wear behavior of multilayered Si-doped DLC films with different thicknesses deposited on different substrates. Figure 6(a) shows the variation of CoF of the film deposited on stainless steel with

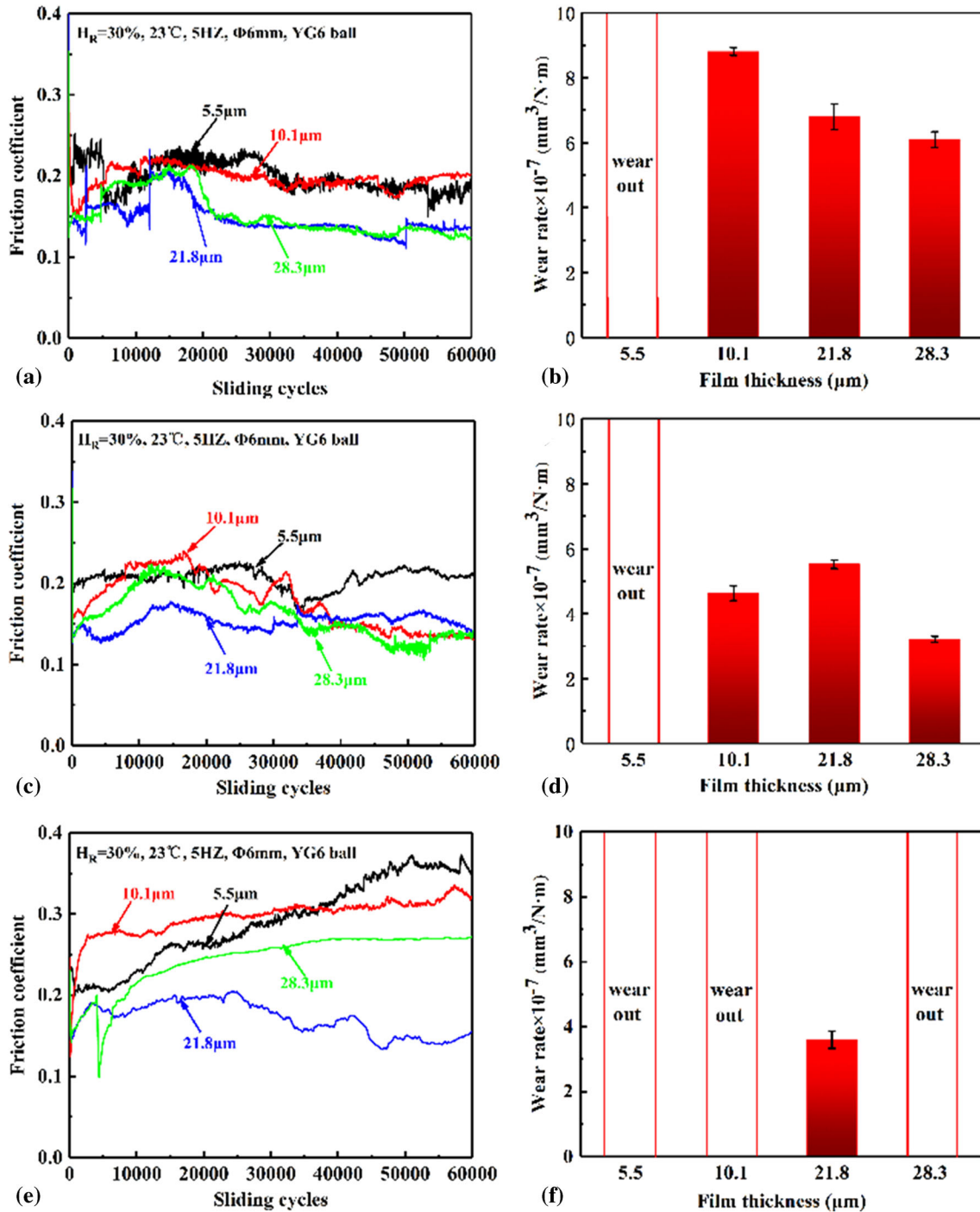


Fig. 6. Friction test results of multilayered Si-doped DLC films: (a, b) stainless steel, (c, d) aluminum alloys and (e, f) copper alloys

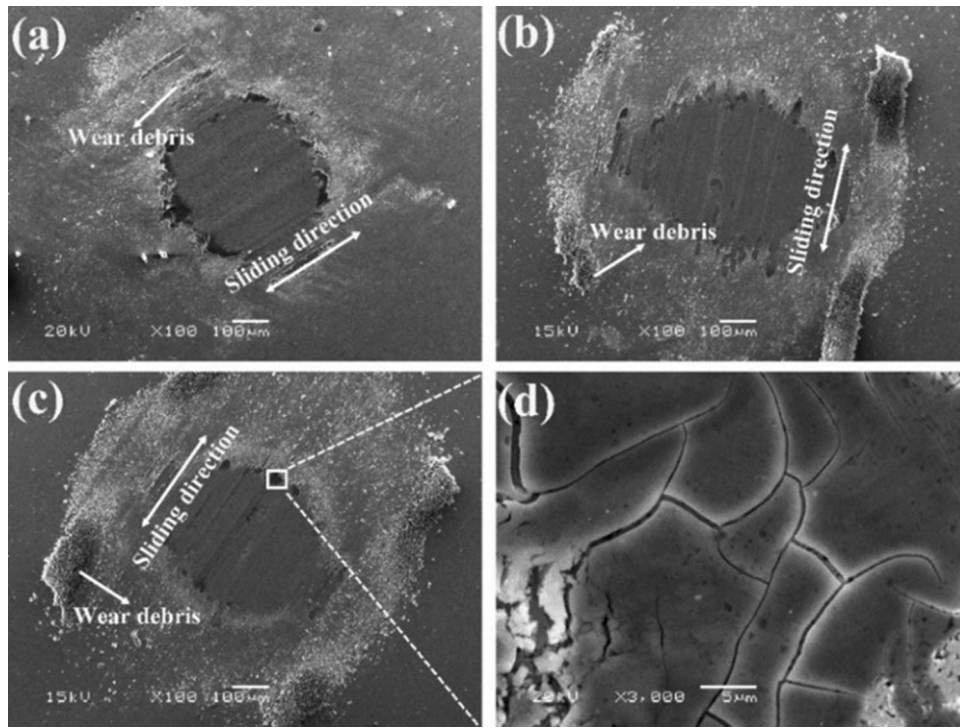


Fig. 7. SEM images of the wear scars on WC balls sliding against multilayered Si-doped DLC films with a thickness of 21.8 μm on different substrates: (a) stainless steel, (b) aluminum alloys, (c) copper alloys and (d) the magnified images of the corresponding white rectangle area in (c)

sliding cycles. The multilayered Si-doped DLC film with a thickness of 5.5 and 10.1 μm after running-in period showed a high CoF of ~ 0.2 . When the film thickness exceeds 10.1 μm , CoF decreases significantly to ~ 0.13 in the steady state. The film having a thickness of 5.5 μm failed after the end of the friction test. Figure 6(b) shows the wear rate results for a multilayered Si-doped DLC film coated on an aluminum alloy. The wear rate of the multilayered Si-doped DLC film with a thickness of 10.1 μm is the highest at $8.8 \times 10^{-7} \text{mm}^3/\text{N m}$. The wear rate decreases to $6.1 \times 10^{-7} \text{mm}^3/\text{N m}$ when the film thickness increases to 28.3 μm . The tribological behavior of the multilayered Si-doped DLC film coated on aluminum alloy substrate is shown in Fig. 6(c) and (d). The running-in period of the film with different thicknesses becomes longer, and fluctuations of CoF are observed even during steady states. Films with a thickness of 5.5 μm also failed after the tribological test. With the increase in the thickness of multilayered Si-doped DLC films, the wear rate of 28.3 μm films is the lowest at $3.2 \times 10^{-7} \text{mm}^3/\text{N m}$. The results are consistent with the adhesion of the multilayered Si-doped DLC films, indicating that the property is one of the factors for adjusting the wear resistance. The wear rate of film deposited on aluminum alloy is lower than that deposited on stainless steel. The CoF of the multilayered Si-doped DLC films coated on copper alloy substrates increases with the sliding cycles except for the relatively low CoF of 21.8 μm thickness (Fig. 6e). The continuous increase in CoF is caused by the rapid wear out of the multilayered Si-doped DLC film on the copper substrate. The wear rate of the multilayered Si-doped DLC film having different thicknesses on copper alloy substrate is shown in Fig. 6(f). Only films having a thickness of 21.8 μm were not worn out and exhibited a relatively low wear rate.

It was found that the multilayered Si-doped DLC films with thicknesses of 5.5 and 10.1 μm on three substrates have relatively high CoF. This can be attributed to the multilayered film having a small thickness which is susceptible to shear failure under normal load compressive stress and thus exhibits higher CoF. As the thickness of the film increases, the residual stress of the film gradually increases. The mismatch between aluminum alloy and carbon produces high internal stress resulting in uneven stress distribution inside the film, resulting in the rise and fluctuation of CoF. The chemical inertness of the Cu element itself and the mismatch between the film result in poor adhesion and poor durability of the multilayered Si-doped DLC film. Furthermore, the good cohesive strength and load-bearing capacity for gradually thickening coating could effectively prevent coating wear during dry sliding. Therefore, the multilayered Si-doped DLC film coated on the copper alloy substrate exhibits poor tribological behavior.

Figure 7 shows the wear scar on WC ball sliding against multilayered Si-doped DLC films with a thickness of 21.8 μm coated on different substrates. In Fig. 7(a), (b) and (c), a small amount of discontinuous transfer film has been formed along the sliding direction on the WC counterpart. Figure 7(d) is the magnified images of the corresponding white rectangle area in Fig. 7(c). The presence of the transfer film can be observed on the WC ball. Figure 8 shows SEM and EDS elemental maps (Si, O and C) for various thicknesses of Si-doped DLC films on WC balls. Previous studies have resulted in Si-doped DLC films that form an oxide lubricant layer during the rubbing process (Ref 41). It can act as a lubricant at the friction interface. It was also found that a plenty of wear debris was generated around the WC counterpart. This can be attributed to the formation of Si oxide during the rubbing process. However,

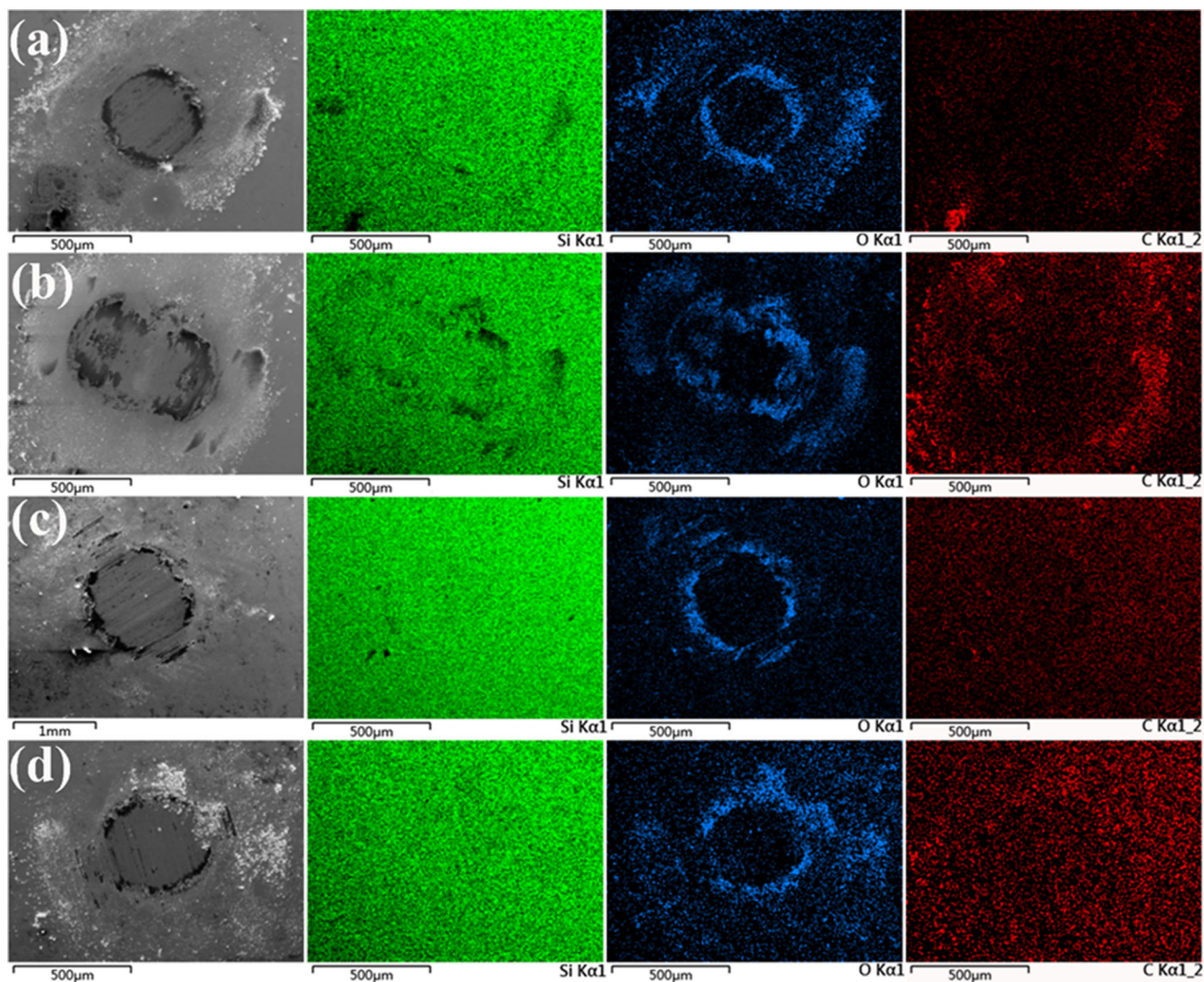


Fig. 8. SEM images and its corresponding EDS elemental mapping of WC balls sliding against multilayered Si-doped DLC films of different thicknesses: (a) 5.5 μm , (b) 10.1 μm , (c) 21.8 μm , (d) 28.3 μm deposited on stainless steel substrates

Table 5 Material properties used in FEM simulations

	Thickness, μm	Ex, GPa	PRXY	D, kg/m^{-3}
304 stainless steel	1500	206	0.26	7930
Aluminum alloy	1500	68	0.33	2710
Copper alloy	1500	123	0.35	8920
Si _x -DLC	0.4	82	0.25	1800
Si _y -DLC	0.2	150	0.25	2200

Ex: Young's modulus (GPa), PRXY: Poisson's ratio, D: Density (kg/m^{-3})

its low hardness can easily peel off the film surface and form wear debris. During repeated friction, it transfers to the surface of the WC ball to form transfer film. The high hardness of the WC ball causes the formed transfer film to be continuously peeled off, so that there is less transfer film on the wear scar.

In order to investigate the difference in wear rate of multilayered Si-doped DLC films on different substrates under the same test conditions, we performed a finite element method (FEM) of the stress distribution of the multilayered Si-doped

DLC films coated on different substrates under the loading condition of the ball indentation system. Schematic diagram of the simulation process system sees reference (Ref 27, 41). The counterpart material is assumed to be a rigid material, and the transition layer was not considered. Assume an axisymmetric system and build half of the geometry to reduce the amount of computation. Material parameters are shown in Table 5.

Figure 9 shows the FEM simulation results for multilayered Si-doped DLC film of 5.5 μm thickness ((Si_x-DLC/Si_y-DLC)₉)

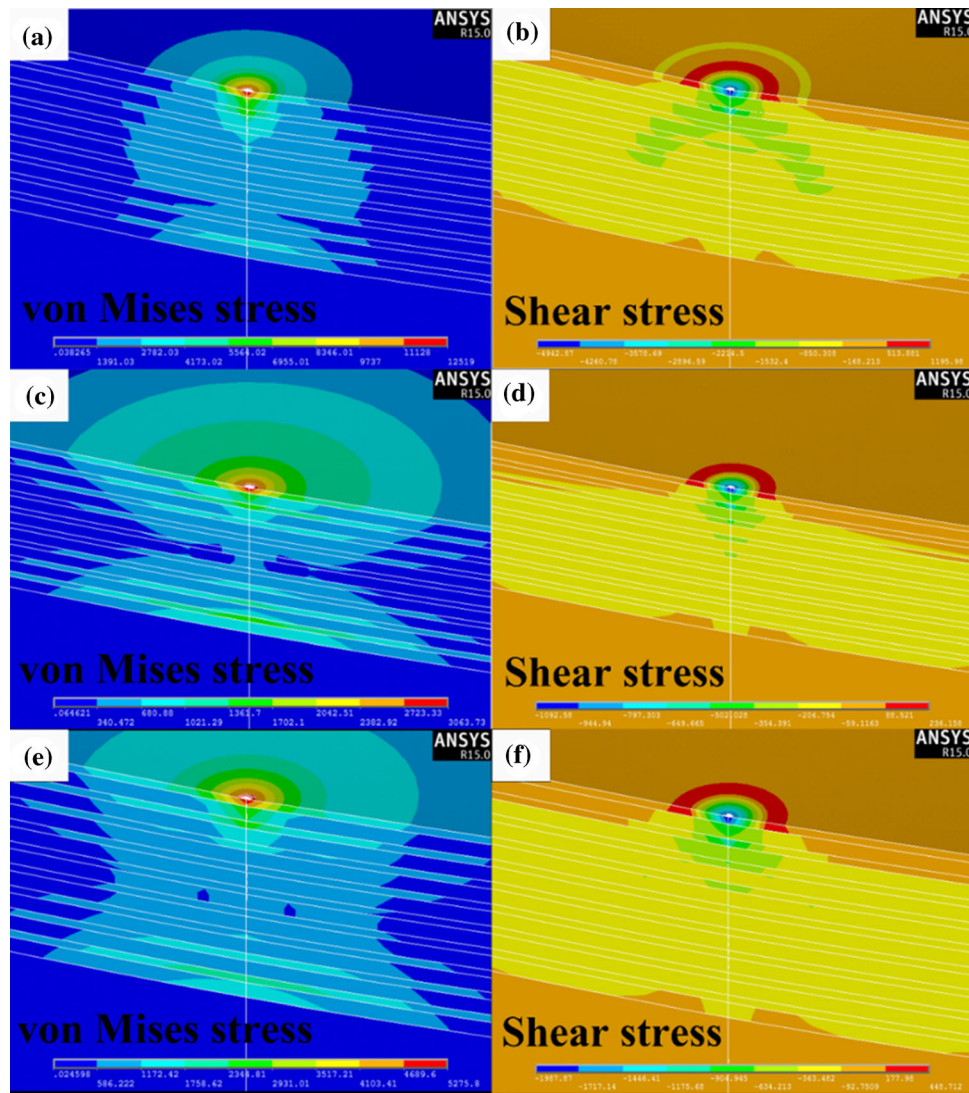


Fig. 9. Contour plots of the von Mises stress and shear stresses for a 5.5- μm multilayered Si-doped DLC system with different substrates: (a, b) stainless steel, (c, d) aluminum alloys and (e, f) copper alloys

Table 6 Maximum von Mises stress and maximum shear stress of multilayered Si-doped DLC films deposited on different substrates with a thickness of 5.5 μm

	Stainless steel	Aluminum alloy	Copper alloy
von Mises stress, GPa	12.51	3.06	5.27
Shear stresses, GPa	1.19	0.23	0.44

on stainless steel, aluminum alloy and copper alloy. First, when a load (150 mN) is applied, the maximum stress is concentrated mainly near the top surface for multilayered Si-doped DLC film system on different substrates. Table 6 lists the maximum von Mises stress and shear stress of multilayered Si-doped DLC film having a thickness of 5.5 μm . The maximum von Mises equivalent stress and corresponding maximum shear stress of the film coated on stainless steel were 12.51 and 1.19 GPa, respectively. Thus, multilayered Si-doped DLC film deposited on aluminum alloy and copper alloy substrate can provide greater stress shielding and prevent substrate wear. Second,

aluminum alloys and copper alloys produce greater stress concentrations at the substrate–film interface than stainless steel substrates. The failure of the substrate–film interface is the most important factor to induce the failure of the film. Therefore, the multilayered Si-doped DLC film has poor adhesion on the aluminum alloy and the copper alloy substrate and is more susceptible to failure. More importantly, the excellent adhesion strength of the multilayered Si-doped DLC film can effectively prevent the film from being worn during the dry-slip process. In addition, different stress fields were observed in the low Si content layer and the high Si content layer due to the difference

of elastic modulus. The difference of stress field between different layers may affect the branching and deflection of cracks at the interface. Therefore, based on the above analysis, the wear resistance of the film on different substrates is related to the contact stress and the adhesion. Effective stress shielding can improve the wear resistance of films on different substrates.

4. Conclusions

In this study, multilayered Si-doped DLC films with thicknesses of 5.5, 10.1, 21.8 and 28.3 μm were deposited on stainless steel, aluminum alloy and copper alloy by PECVD techniques. The main results discussed from the above are as follows:

- (1) The interaction between the compressive-stressed Si_x -DLC and the tensile-stressed Si_y -DLC can reduce the internal stress, and the continuous growth of the multilayered Si-doped DLC film can be successfully performed on SUS 304 stainless steel, 3004 aluminum alloy and T3 copper alloy.
- (2) The results of nanoindentation tests show that the hardness of multilayered Si-doped DLC film on the stainless steel and aluminum alloy substrates increased with deposition time. However, the high mismatch interface between the carbon and the copper atoms, resulting in the multilayered Si-doped DLC film having a thickness of more than 10 μm on the copper alloy substrate, was partially peeled off. Therefore, a large internal stress release reduces the hardness of the film.
- (3) During the scratch test, the adhesion of multilayered Si-doped DLC film on stainless steel, aluminum and copper alloy substrates increased with film thickness. The multilayered Si-doped DLC film on the copper alloy substrates shows poor adhesion strength induced dominantly by the high mismatch interface between the carbon and the copper atoms.
- (4) The sliding friction test also shows that the film with a smaller thickness ($< 20 \mu\text{m}$) is prone to shear deformation and the friction coefficient is increased. The fluctuation and increase in the coefficient of friction can be attributed to the uneven distribution of internal stress and surface deformation. The stress shielding and adhesion determine the wear resistance of the multilayered Si-doped DLC film on different substrates.

Acknowledgments

This work was supported by National Key R&D Program of China (No. 2018YFB0703801) and the National Natural Science Foundation of China (Nos. 51775535, 11972344).

References

1. H. Maruno and A. Nishimoto, Adhesion and Durability of Multi-layered Diamond-like Carbon Films Deposited on Aluminum Alloy, *Surf. Coat. Tech.*, 2018, **354**, p 134–144

2. S.D.A. Lawes, M.E. Fitzpatrick, and S.V. Hainsworth, Evaluation of the Tribological Properties of DLC for Engine Applications, *J. Phys. D Appl Phys.*, 2007, **40**, p 5427–5437
3. S.R. Polaki, N. Kumar, N.G. Krishna, K. Madapu, M. Kamruddin, S. Dash, and A.K. Tyagi, Microwave Plasma Induced Surface Modification of Diamond-Like Carbon Films, *Surf. Topogr. Metrol. Prop.*, 2017, **5**, p 045005
4. J. Robertson, Diamond-like Amorphous Carbon, *Mat. Sci. Eng. R*, 2002, **37**, p 129–281
5. M. Goto, Preparations and Tribological Properties of Soft-metal/DLC Composite Coatings by RF Magnetron Sputter Using Composite Targets, *Int. J. Mech. Mater. Des.*, 2017, **14**, p 313–327
6. B.C. Yeldose and B. Ramamoorthy, Characterization of DC Magnetron Sputtered Diamond-Like Carbon (DLC) Nano Coating, *Int. J. Adv. Manuf. Technol.*, 2007, **38**, p 705–717
7. S. Grigoriev, M. Volosova, S. Fyodorov, M. Lyakhovetskiy, and A. Seleznev, DLC-coating Application to Improve the Durability of Ceramic Tools, *J. Mater. Eng. Perform.*, 2019, **28**, p 4415–4426
8. Y. Sun, X.Y. Huang, and H. Wang, Influence of Hydrogen Content on Optical and Mechanical Performances of Diamond-Like Carbon Films on Glass Substrate, *J. Mater. Eng. Perform.*, 2016, **25**, p 1570–1577
9. M. Odén, J. Almer, and G. Håkansson, The Effects of Bias Voltage and Annealing on the Microstructure and Residual Stress of Arc-Evaporated Cr-N Coatings, *Surf. Coat. Tech.*, 1999, **120–121**, p 272–276
10. A. Leyland and A. Matthews, Thick TiTiN Multilayered Coatings for Abrasive and Erosive Wear Resistance, *Surf. Coat. Tech.*, 1994, **70**, p 19–25
11. Y. Ye, S. Jia, D. Zhang, W. Liu, and H. Zhao, A Study for Anticorrosion and Tribological Behaviors of Thin/Thick Diamond-Like Carbon Films in Seawater, *Surf. Topogr. Metrol. Prop.*, 2018, **6**, p 014004
12. Q. Wei, A.K. Sharma, J. Sankar, and J. Narayan, Mechanical Properties of Diamond-Like Carbon Composite Thin Films Prepared by Pulsed Laser Deposition, *Compos. Part B*, 1999, **30**, p 675–684
13. S. Logothetidis, M. Gioti, C. Charitidis, P. Patsalas, J. Arvanitidis, and J. Stoemenos, Stability, Enhancement of Elastic Properties and Structure of Multilayered Amorphous Carbon Films, *Appl. Surf. Sci.*, 1999, **138–139**, p 244–249
14. P. Wang, X. Wang, T. Xu, W.M. Liu, and J. Zhang, Comparing Internal Stress in Diamond-Like Carbon Films with Different Structure, *Thin Solid Films*, 2007, **515**, p 6899–6903
15. S. Neuville and A. Matthews, A Perspective on the Optimisation of Hard Carbon and Related Coatings for Engineering Applications, *Thin Solid Films*, 2007, **515**, p 6619–6653
16. A. Leyland and A. Matthews, On the Significance of the H-E Ratio in Wear Control: A Nanocomposite Coating Approach to Optimised Tribological Behavior, *Wear*, 2000, **246**, p 1–11
17. L.L. Liu, Z.Z. Wu, X.K. An, S. Xiao, S.H. Cui, H. Lin, R.K.Y. Fu, X.B. Tian, R.H. Wei, P.K. Chu, and F. Pan, Excellent Adhered Thick Diamond-Like Carbon Coatings by Optimizing Hetero-Interfaces with Sequential Highly Energetic Cr and C Ion Treatment, *J. Alloy. Compd.*, 2018, **735**, p 155–162
18. J. Sun, Z. Fu, W. Zhang, C. Wang, W. Yue, S. Lin, and M. Dai, Friction and Wear of Cr-Doped DLC Films Under Different Lubrication Conditions, *Vacuum*, 2013, **94**, p 1–5
19. E.D. Rejowski, M.C.L. de Oliveira, R.A. Antunes, and M.F. Pillis, Structural Characterization and Corrosion Stability of a Si-Doped DLC Coating Applied on Cylinder Liner, *J. Mater. Eng. Perform.*, 2014, **23**, p 3926–3933
20. S. Viswanathan, L. Mohan, P. Bera, V.P. Kumar, H.C. Barshilia, and C. Anandan, Corrosion and Wear Behaviors of Cr-Doped Diamond-Like Carbon Coatings, *J. Mater. Eng. Perform.*, 2017, **26**, p 3633–3647
21. E.Z. Carvalho, B.J. Kooi, and J.Th.M. De Hosson, Stress Analysis and Microstructure of PVD Monolayer TiN and Multilayer TiN/(Ti, Al)N Coatings, *Thin Solid Films*, 2003, **429**, p 179–189
22. M. Lorenz, V. Lazenka, P. Schwinkendorf, F. Bern, M. Ziese, H. Modarresi, and A. Volodin, Multiferroic BaTiO₃-BiFeO₃ Composite Thin Films and Multilayers: Strain Engineering and Magnetoelectric Coupling, *J. Phys. D Appl Phys.*, 2014, **47**, p 135303
23. Y.Q. Wei, X.Y. Zong, Z.Q. Jiang, and X.B. Tian, Characterization and Mechanical Properties of TiN/TiAlN Multilayer Coatings with Different Modulation Periods, *Int. J. Adv. Manuf. Technol.*, 2017, **96**, p 1677–1683

24. T. Takeshita, Y. Kurata, and S. Hasegawa, Bonding Properties of Glow-Discharge Polycrystalline and Amorphous Si-C Films Studied by X-Ray Diffraction and X-Ray Photoelectron Spectroscopy, *J. Appl. Phys.*, 1992, **71**, p 5395–5400
25. T.F. Zhang, Z.X. Wan, J.C. Ding, S.H. Zhang, Q.M. Wang, and K.H. Kim, Microstructure and High-Temperature Tribological Properties of Si-Doped Hydrogenated Diamond-like Carbon Films, *Appl. Surf. Sci.*, 2018, **435**, p 963–973
26. M.J. Cui, J.B. Pu, J. Liang, L.P. Wang, G.A. Zhang, and Q.J. Xue, Corrosion and Tribocorrosion Performance of Multilayer Diamond-Like Carbon Film in NaCl Solution, *RSC Adv.*, 2015, **5**, p 104829–104840
27. J.J. Wang, J.B. Pu, G.A. Zhang, and L.P. Wang, Interface Architecture for Superthick Carbon-Based Films Toward Low Internal Stress and Ultrahigh Load-Bearing Capacity, *ACS Appl. Mater. Interface*, 2013, **5**, p 5015–5024
28. D. César, R. Tello, E. Broitman, F.J. Flores-Ruiz, O. Jiménez, and M. Flores, Mechanical Properties and Tribological Behavior at Micro and Macro-Scale of WC/WCN/W Hierarchical Multilayer Coatings, *Tribol. Int.*, 2016, **101**, p 194–203
29. J.J. Wang, J.B. Pu, G.A. Zhang, and L.P. Wang, Tailoring the Structure and Property of Silicon-Doped Diamond-Like Carbon Films by Controlling the Silicon Content, *Surf. Coat. Tech.*, 2013, **235**, p 326–332
30. J.B. Pu, J.J. Wang, D.Q. He, and S. Wan, Corrosion and Tribocorrosion Behaviour of Super-Thick Diamond-Like Carbon Films Deposited on Stainless Steel in NaCl Solution, *Surf. Interface Anal.*, 2016, **48**, p 360–367
31. Y.Y. Lin, Z.F. Zhou, and K.Y. Li, Improved Wear Resistance at High Contact Stresses of Hydrogen-Free Diamond-Like Carbon Coatings by Carbon/Carbon Multilayer Architecture, *Appl. Surf. Sci.*, 2017, **477**, p 137–146
32. A. Modabberasl, P. Kameli, M. Ranjbar, H. Salamati, and R. Ashiri, Fabrication of DLC Thin Films with Improved Diamond-Like Carbon Character by the Application of External Magnetic Field, *Carbon*, 2015, **94**, p 485–493
33. A.C. Ferrari and J. Robertson, Interpretation of Raman Spectra of Disordered and Amorphous Carbon, *Phys. Rev. B*, 2000, **61**, p 14095
34. R. Paul, S.N. Das, S. Dalui, R.N. Gayen, R.K. Roy, R. Bhar, and A.K. Pal, Synthesis of DLC Films with Different sp²/Sp³ratios and Their Hydrophobic Behaviour, *J. Phys. D Appl Phys*, 2008, **41**, p 055309
35. R. Cruz, J. Rao, T. Rose, K. Lawson, and J.R. Nicholls, DLC–Ceramic Multilayers for Automotive Applications, *Diam. Relat. Mater.*, 2006, **15**, p 2055–2060
36. Z. Li, Y. Wang, X. Cheng, Z. Zeng, J. Li, X. Lu, L. Wang, and Q. Xue, Continuously Growing Ultrathick CrN Coating to Achieve High Load-Bearing Capacity and Good Tribological Property, *ACS Appl. Mater. Interface.*, 2018, **10**, p 2965–2975
37. J. Musil and M. Jirout, Toughness of Hard Nanostructured Ceramic Thin Films, *Surf. Coat. Tech.*, 2007, **201**, p 5148–5152
38. N. Konkunthot, P. Photongkam, and P. Wongpanya, Improvement of Thermal Stability, Adhesion Strength and Corrosion Performance of Diamond-like Carbon Films with Titanium Doping, *Appl. Surf. Sci.*, 2019, **469**, p 471–486
39. X.Z. Ding, B.K. Tay, S.P. Lau, P. Zhang, and X.T. Zeng, Structural and Mechanical Properties of Ti-Containing Diamond-Like Carbon Films Deposited by Filtered Cathodic Vacuum Arc, *Thin Solid Films*, 2002, **408**, p 183–187
40. J. Zhang, X. Yu, X.A. Zhao, and L. Zhang, Influences of Interfacial Carbonization on the Structure and Mechanical Properties of Multilayered Cr-Containing Diamond-Like Carbon Films, *J. Phys. Chem. C*, 2017, **121**, p 6781–6787
41. J.J. Wang, J.B. Pu, G.A. Zhang, and L.P. Wang, Architecture of Superthick Diamond-Like Carbon Films with Excellent High Temperature Wear Resistance, *Tribol. Int.*, 2015, **81**, p 129–138

Publisher's Note Springer Nature remains neutral with regard to jurisdictional claims in published maps and institutional affiliations.